Effects of Ti addition on the soft magnetic properties of Fe - N films

1997 J. Phys.: Condens. Matter 9 8443

(http://iopscience.iop.org/0953-8984/9/40/011)

J. Phys.: Condens. Matter **9** (1997) 8443–8451. Printed in the UK PII: S0953-8984(97)82858-5

Effects of Ti addition on the soft magnetic properties of Fe–N films

H Y Wang, E Y Jiang, H L Bai, P Wu, Y Wang and F F Gong
Department of Applied Physics, Tianjin University, Tianjin, 300072, People's Republic of China

Received 24 March 1997, in final form 28 May 1997

Abstract. FeTiN films with good soft magnetic properties were prepared on Si and NaCl single-crystal substrates by facing-targets sputtering (FTS). The effects of Ti addition on the structural and magnetic properties of Fe–N films were investigated. Ti has been found effective in improving the soft magnetic properties as well as the thermal stability of FeN films. For the films containing 5–12 at.% Ti prepared under sputtering conditions of $pN_2 = 0.04$–0.07 Pa, a substrate temperature of 100 °C, and a sputtering rate of 0.2 nm s^{-1}, the following properties are observed: very high saturation magnetization $4\pi M_s$ (2.3–2.5 T), low coercivity H_c (160–240 A m^{-1}), and high relative permeability μ (3000–3500 at 1 MHz). The thermal stability of these films was also found to be good, e.g. H_c was less than 240 A m^{-1} and $4\pi M_s$ was higher than 2.3 T for the films annealed up to 500 °C. The crystal structures of the FeTiN films were examined with an x-ray diffractometer and a transmission electron microscope. Ti addition affects the formation of magnetic iron nitride phases and makes the crystallites small. The fine-grained Fe–N phase, together with finely dispersed TiN precipitates, is considered to be one of the main factors responsible for the good magnetic properties and thermal stability.

1. Introduction

A lot of attention has recently been focused on Fe–N films, because of their excellent magnetic properties, and their significantly improved corrosion and wear resistance over that of pure iron. α''-$Fe_{16}N_2$ is one of the most attractive magnetic materials since it has very large saturation magnetization, as large as 2.8–3.0 T [1–9]. Given the need for soft properties, it seems likely that the film of this phase may be useful as a magnetic layer of magnetic heads for high-density recording. Moreover, better thermal stability of soft magnetism is also required. Various types of Fe–N film with both single-layer [10] and multiphase gradient films [11] have been investigated. Although the Fe–N film has a very high flux density, it has the disadvantages of high magnetostriction and poor thermal magnetic properties. The addition of a third element to form ternary Fe–M–N films (M = Ta, Zr, Hf, Nb) [12–14] has met with success in solving the soft magnetic and thermal problems. However, systematic study of the effect of Ti addition on the soft magnetic properties and thermal stability of Fe–N films has not been reported yet.

This paper reports the effect of Ti addition on the soft magnetic properties and the thermal stability of Fe–N films. FeTiN films with 0–30 at.% Ti concentrations were prepared using a facing-targets sputtering system. We have newly found that appropriate Ti addition can not only improve the soft magnetic properties of Fe–N films, but also enhance the thermal stability of the soft magnetic properties.

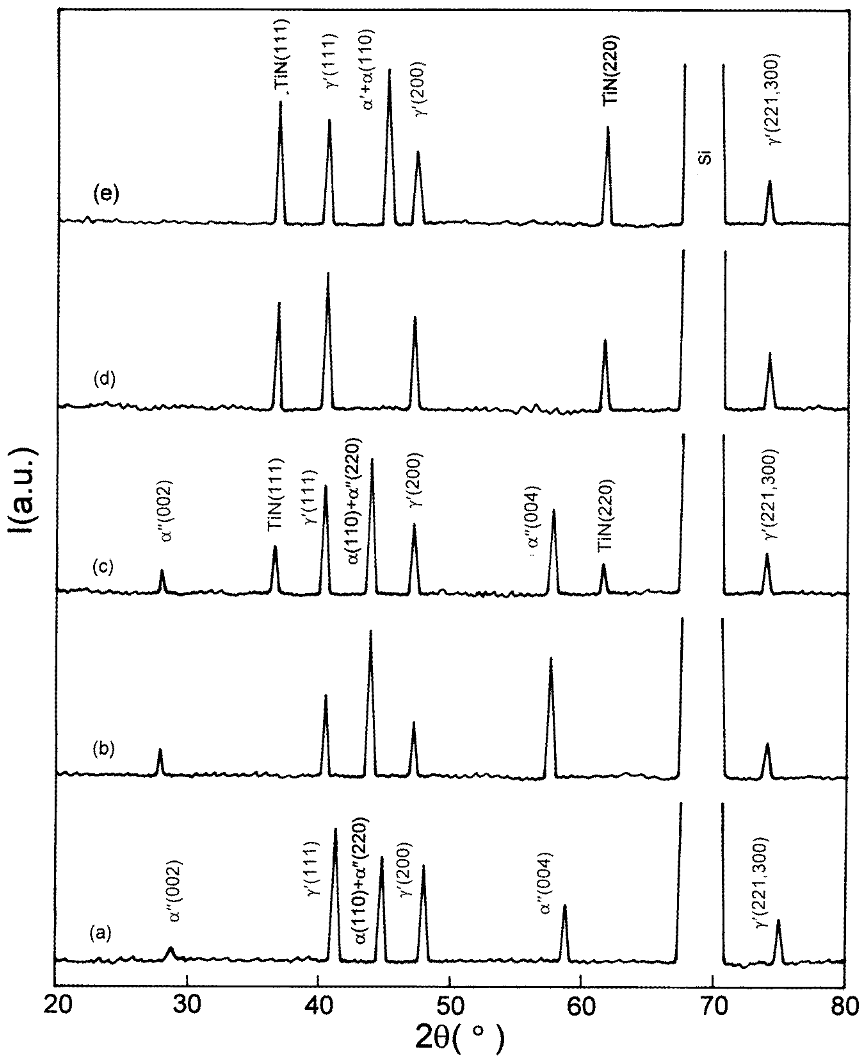

Figure 1. X-ray diffraction patterns of FeTiN films with various Ti concentrations: (a) 0 at.%; (b) 5 at.%; (c) 10 at.%; (d) 25 at.%; and (e) 35 at.%

2. Experiment

FeTiN films with 0–30 at.% Ti concentrations were prepared by facing-targets sputtering (FTS) on both Si and NaCl single-crystal substrates. The sputtering targets are composite materials consisting of 10 mm $\times$ 4 mm Ti chips placed on $\varnothing$100 mm $\times$ 50 mm Fe (99.99%) targets. The sputtering gas and reactive gas were Ar (99.99%) and N_2 (99.99%) respectively. After the chamber was evacuated to a base pressure of 6×10^{-5} Pa, argon gas was introduced. During sputtering, the Ar gas pressure and N_2 gas pressure were kept constant at 0.3 Pa and 0.04–0.07 Pa, respectively. The composition of the FeTiN films was adjusted by varying the number of Ti chips mounted on iron targets. The substrate temperature was held at 100 °C. The deposition rate was about 0.2 nm s^{-1}. The thickness of the film was about 50 nm.

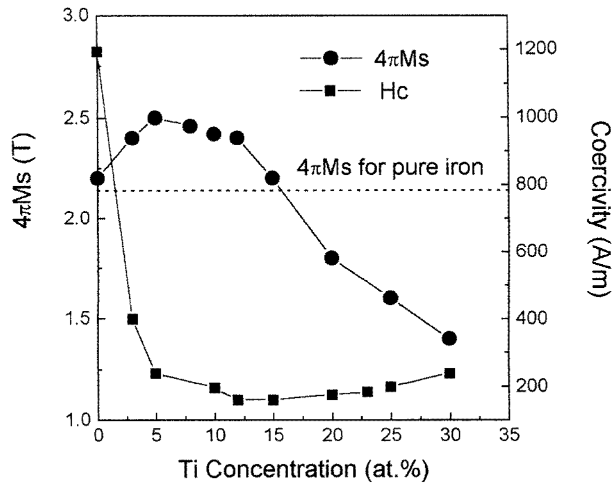

Figure 2. The dependences of the saturation magnetization $4\pi M_s$ and coercivity H_c on the Ti concentrations of FeTiN films.

The crystal structures of the as-deposited and annealed (Fe, Ti)–N films were examined with an x-ray diffractometer (XRD) using Cu Kα radiation and a JEM-200CX transmission electron microscope capable of energy-dispersive x-ray analysis. The saturation magnetization $4\pi M_s$ and coercivity H_c were measured with a vibrating-sample magnetometer with a resolution of 2×10^{-6} emu in a magnetic field of 8 kOe which was applied parallel to the sample plane at room temperature. The relative permeability μ was measured by a permeability measurement system. The thickness of the film was measured by the multibeam interference technique. The composition was evaluated using electron probe analysis.

3. Results and discussion

Figure 1 shows x-ray diffraction patterns of FeTiN films with various Ti concentrations. The FeTiN films with Ti concentrations of 0–10 at.% contain α''-$Fe_{16}N_2$ phase and γ'-Fe_4N phase. For the 5 at.% Ti films, the intensities of the α''-$Fe_{16}N_2$ peaks are larger than those of the γ'-Fe_4N peaks, showing that the α''-phase is the dominant phase in the film. The volume fraction of the α''-phase estimated from XRD was 36–40 vol% for Ti-free film and 74–76 vol% for the 5 at.% Ti film. There is no evidence of Ti or Ti–N compounds in the XRD pattern of the 5 at.% Ti sample. Ti atoms apparently dissolve substitutionally in the bcc Fe lattice. This illustrates why in XRD patterns the positions of the α''(002), (220), (004) and γ'(111), (200) peaks of the 5 at.% Ti sample shift to low 2θ-values (the lattice expands) compared with those of the Ti-free sample. A small volume fraction of TiN phase would be difficult to detect by means of XRD. In the XRD pattern of the 10 at.% Ti sample, TiN phase appears. As the Ti concentration increases to 25 at.%, the α''-phase disappears, the intensities of TiN and γ'-peaks increase, showing that the TiN and γ'-phases are the dominant phases in this film. When the Ti concentration is 30 at.%, α-Fe peaks appear, and the intensities of the γ'-peaks decrease while those of the TiN peaks increase. The grain size is measured from the transmission electron microscope bright-field images. In the Ti-free case, the grain size is about 10–15 nm; it decreases abruptly with Ti addition, and reaches a minimum value of about 3–5 nm at 10–30 at.% Ti. As TiN has a higher melting point, it would be preferable to suppress the crystallite growth at high temperatures in the preparation process by TiN creation in FeTiN films.

Figure 2 shows the saturation magnetization $4\pi M_s$ and coercivity H_c as functions of the Ti concentrations of FeTiN films. The FeTiN films exhibit very high values of $4\pi M_s$ of 2.3–2.5T and a low coercivity H_c of 160–240 A m^{-1} at Ti concentrations of about 5–12 at.%. From the XRD patterns, one can see that the films with 5–12 at.% Ti contain a large amount of α''-phase, which exhibits high saturation magnetization. H_c for the Ti-free film is larger than that of the Ti-containing film, because the grain size is larger in the Ti-free film, and Ti addition in the films made the crystallites small. In the region of a high Ti concentration exceeding 15 at.%, $4\pi M_s$ shows a relatively low value, because the γ'-phase ($4\pi M_s = 1.8$ T) and the TiN phase (non-magnetic) are the dominant phases in these films.

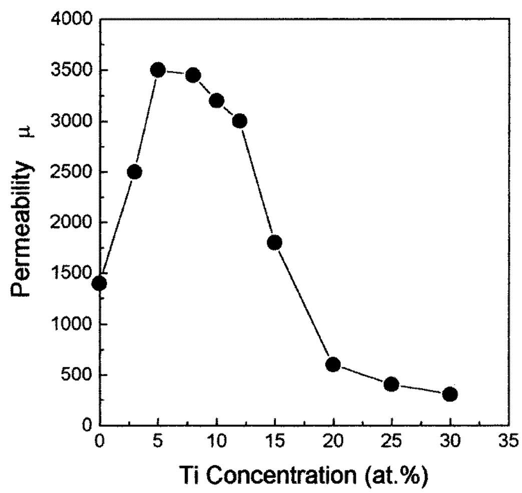

Figure 3. The dependence of the relative permeability μ on the Ti concentrations of FeTiN films.

Table 1. The magnetic properties and the thermal stability temperatures (T_s) of FeTiN, FeMN (M = Ta, Hf), and FeZrCN films.

	FeTiN	FeTaN	FeHfN	FeZrCN
$4\pi M_s$ (T)	2.3–2.5	1.4–1.7	1.2–1.5	1.6–1.7
H_c (A m^{-1})	160–240	8–160	24	5
μ	3000–3500 (1 MHz)	3000–4500	1700 (100 MHz)	2750 (1 MHz)
T_s (°C)	500	500–550	500	600
Reference		[12]	[13]	[14]

Figure 3 shows the dependence of the relative permeability μ on the Ti concentrations of FeTiN films. μ increases with the Ti concentration, reaching a maximum value of about 3500 at 5–8 at.% Ti concentration, and then decreases to 3000 with the increase of the Ti concentration to 12 at.%; a further increase of the Ti concentration results in a rapid decrease in μ, and μ is only 400–500 at 25–30 at.% Ti. This suggests that there is a preferrred range of Ti concentration for FeTiN films for obtaining good soft magnetic properties. This is

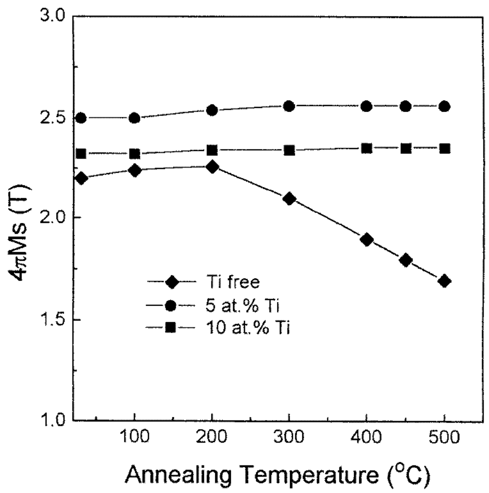

Figure 4. The dependence of $4\pi M_s$ on the annealing temperature for films with three typical Ti concentrations.

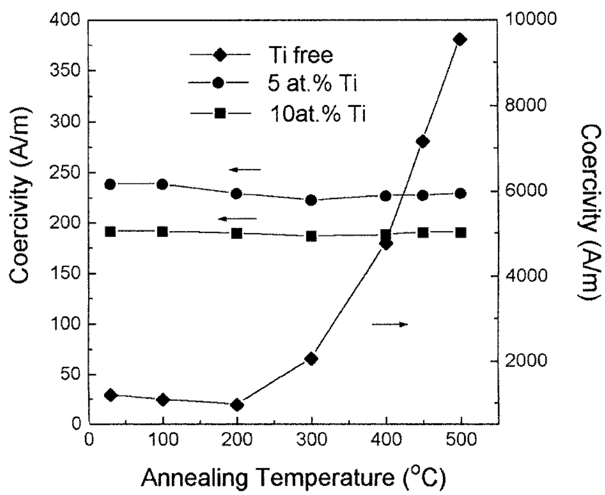

Figure 5. The dependence of H_c on the annealing temperature for films with three typical Ti concentrations.

explained as follows. In the preparation process of FeTiN films, some Ti atoms dissolve substitutionally in the bcc Fe lattice and occupy the sites of Fe atoms, and others have a tendency to form the nitride TiN. The TiN compound is likely to play an important role in the microstructure.

Figure 4 and figure 5 show the variations of $4\pi M_s$ and H_c with the annealing temperature (T_a) for films with three typical Ti concentrations (0 at.%, 5 at.%, 10 at.%), respectively. The films with Ti concentrations of 5 at.% and 10 at.% show good thermal stability, H_c being less than 240 A m^{-1} and $4\pi M_s$ being higher than 2.3 T for the two films annealed up to 500 °C. However, the magnetic softness of the Ti-free film is not good over the entire temperature range. For the Ti-free film, $4\pi M_s$ shows a rapid decrease while H_c shows a rapid increase when the annealing temperature is higher than 300 °C.

A comparison of the magnetic properties such as $4\pi M_s$, H_c, μ, and the thermal stability for FeTiN films to those for FeMN (M = Ta, Hf) and FeZrCN films is listed in table 1. $4\pi M_s$ is larger for FeTiN films than for FeMN (M = Ta, Hf) and FeZrCN films, and the

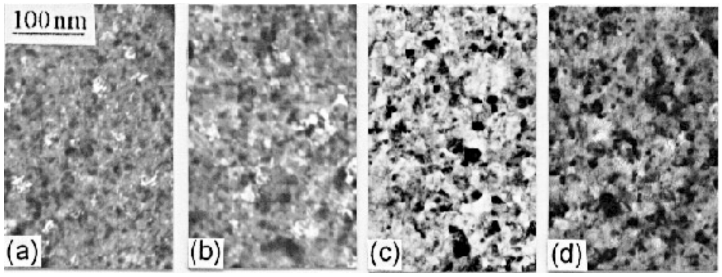

Figure 6. TEM images of Ti-free film (a) as deposited, (b) with $T_a = 300$ °C, (c) with $T_a = 400$ °C, and (d) with $T_a = 500$ °C.

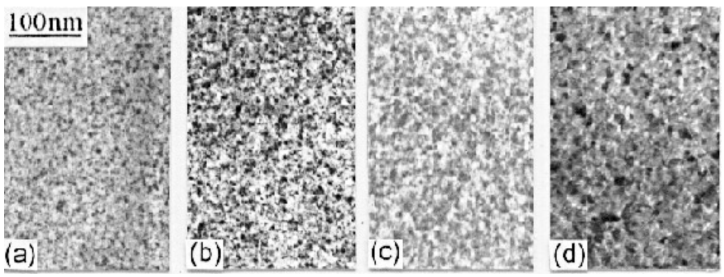

Figure 7. TEM images of 5 at.% Ti films (a) as deposited, (b) with $T_a = 300$ °C, (c) with $T_a = 400$ °C, and (d) with $T_a = 500$ °C.

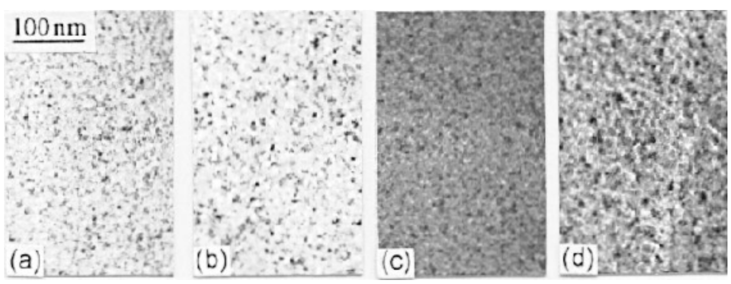

Figure 8. TEM images of 10 at.% Ti films (a) as deposited, (b) with $T_a = 300$ °C, (c) with $T_a = 400$ °C, and (d) with $T_a = 500$ °C.

soft magnetic properties and the thermal stability of FeTiN films are as good as those of FeMN (M = Ta, Hf) and FeZrCN films.

Figure 6, figure 7, and figure 8 show the transmission electron microscope images of FeTiN films with Ti concentrations of 0 at.%, 5 at.%, and 10 at.%, respectively, as deposited, and for annealing temperatures of 300 °C, 400 °C, and 500 °C. For the Ti-free film, the crystallite size was 10–15 nm in the as-deposited film. Following 400 °C and 500 °C annealing, large crystallites are observed, and, as shown in figure 2, H_c increases markedly. For the 5 at.% and 10 at.% Ti films, the grain size is about 3–5 nm in the as-deposited films. Annealing at 500 °C for 30 minutes causes only a small increase in grain size. The crystallite size is smaller than 10 nm for the two films annealed at 500 °C. The existence of TiN in the film seems to suppress the crystallite growth and the phase transformation of Fe–N compounds at a higher annealing temperature. Ti addition in Fe–N films makes

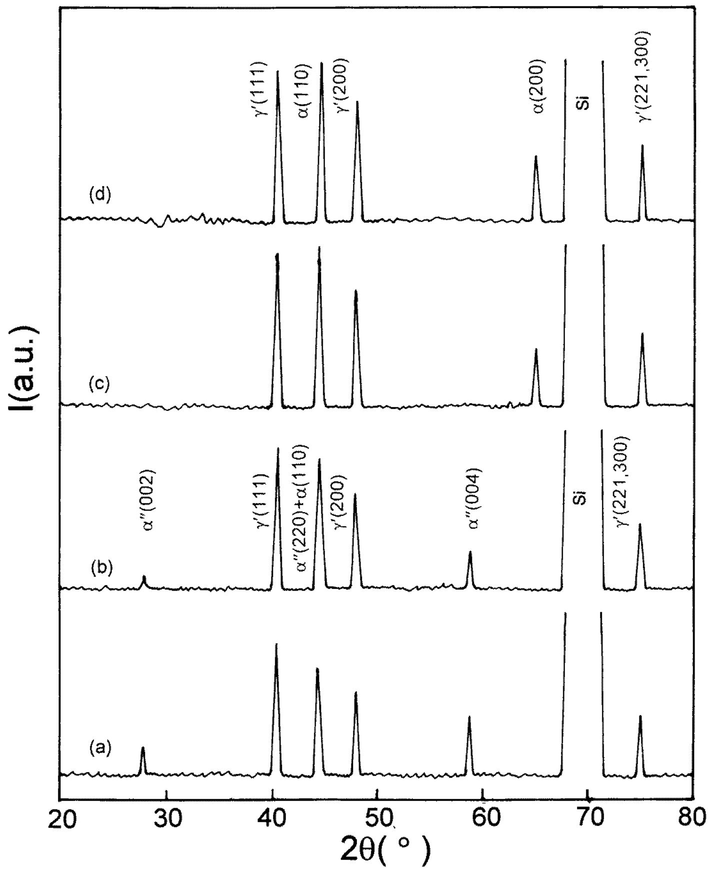

Figure 9. X-ray diffraction patterns of Ti-free films as functions of the annealing temperature, (a) as deposited, (b) with $T_a = 300$ °C, (c) with $T_a = 400$ °C, and (d) with $T_a = 500$ °C.

the crystallites fine, and fine crystal structure is one of the most important origins of soft magnetism of FeTiN films.

Figure 9 shows x-ray diffraction patterns of Ti-free film as functions of the annealing temperature. The structural changes with annealing temperature are distinct. At $T_a = 300$ °C, the intensities of α''-phase decrease while those of γ'-phase increase compared with those for the as-deposited film. At $T_a = 400$ °C, the α''-phase disappears, α-Fe phase appears, and the intensity of the γ'-phase increases in the XRD pattern, showing that the α''-phase has decomposed into α-Fe and the γ'-phase. This result is in agreement with those reported by Kim and Takahashi [1] and Jack [15]. The change in structure from α''-phase to γ'-phase at $T_a = 300$–400 °C is the cause of the decrease in $4\pi M_s$, as shown in figure 4. The structures of FeTiN films with 5 at.% and 10 at.% Ti show good thermal stability, as shown in figure 10. At $T_a = 500$ °C, α''-peaks still exist for the two samples, showing that Ti addition can improve the thermal stability of α''-phase. This is why the value of $4\pi M_s$ for these films is higher than 2.3 T at $T_a = 500$ °C.

In order to determine accurate lattice constants a and c for the α''-$(\mathrm{Fe, Ti})_{16}\mathrm{N}_2$ phase of the FeTiN samples, the lattice constants a and c calculated for each plane are plotted

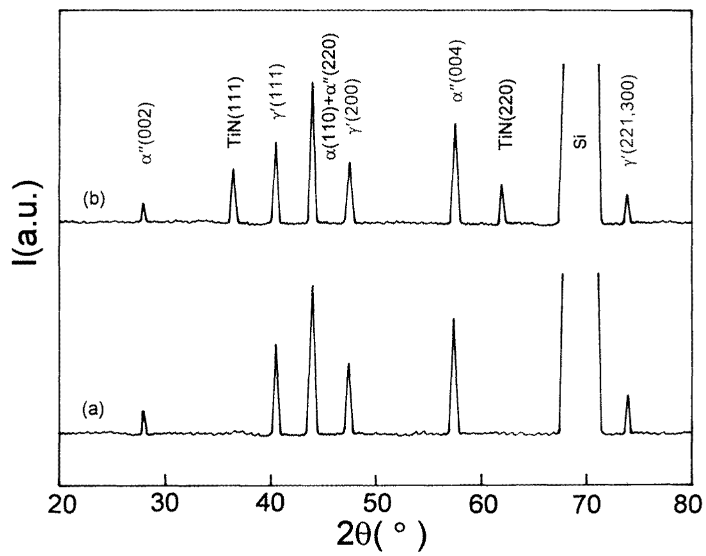

Figure 10. X-ray diffraction patterns of FeTiN films annealed at $T_a = 500$ °C containing (a) 5 at.% Ti and (b) 10 at.% Ti.

against the Nelson–Riley function

$$\cos^2\theta/\sin\theta + \cos^2\theta/\theta.$$

The extrapolated values of the lattice constant $a = 0.613 \pm 0.012$ nm and $c = 0.632 \pm 0.002$ nm for α''-$(Fe, Ti)_{16}N_2$ phase are somewhat larger than those of the α''-$Fe_{16}N_2$ precipitates in bulk powder reported by Jack [15]. This difference indicates that the bct structure of Ti-containing α''-phase was expanded along both the *a*- and the *c*-axes, so the interstitial sites are wider in the Fe–Ti lattice than in the Fe lattice. This suggests that some Fe atom positions are occupied by Ti atoms. The 16:2 nitride is considered to be a nitrogen-ordered form of the tetragonal Fe–N solid solution, which is derived without changing the basic arrangement of Fe atoms in the bcc structure. Therefore, it can be speculated that the Ti-containing 16:2 nitride also forms with less strain energy, leading to a higher stability. The better stability of Ti-containing α''-phase may be caused by Ti addition.

For the 10–12 at.% Ti sample, the enhanced thermal stability of α''-phase in the FeTiN films could be related to the presence and formation of TiN phase. Kopcewicz *et al* [16] suggested that the presence of the alloying element Ti influences the thermal stability of nitrides in two ways:

(1) by increasing the binding energy of nitrides, thus limiting the release of nitrogen from nitrides; and

(2) by forming traps for released nitrogen atoms, which lead to the formation of TiN nitrides.

In the latter case, the cause for the increased stability of nitrides will be the slower nitrogen migration.

Table 2. The dependence on Ti concentration of the fractions of phases, grain size, magnetic properties, and thermal stability temperature of FeTiN films.

Ti concentration (at.%)		0	5	10
Fraction of phase (vol. %)	α''	36–40	74–76	65–67
	γ'	60–64	24–26	28–30
	TiN	0	0	4–6
Grain size (nm)		10–15	3–5	3-5
$4\pi M_s$ (T)		2.2	2.5	2.4
H_c (A m^{-1})		1120	240	160
μ(1 MHz)		1400	3500	3200
Thermal stability temperature (°C)		350	500	500

4. Conclusion

The effects of Ti addition on the soft magnetic and structural properties of Fe–N films were investigated. Ti has been found effective in improving the soft magnetic properties as well as the thermal stability of FeN films. The results are listed in table 2. Ti addition affects the formation of magnetic iron nitride phases and makes the crystallites small. The fine-grained Fe–N phase, together with finely dispersed TiN precipitates, is considered to be one of the main factors as regards achieving good magnetic properties and thermal stability.

Acknowledgments

This work is supported in part by the National Natural Science Foundation of China. The authors are grateful to Dr Y P Wang and others in the TEM Laboratory of Peking University.

References

[1] Kim T K and Takahashi M 1972 *Appl. Phys. Lett.* **20** 492
[2] Nakajima K, Okamoto S and Okada T 1989 *J. Appl. Phys.* **65** 4357
[3] Komuro M, Kozono Y, Hanazono M and Sugita Y 1990 *J. Appl. Phys.* **67** 5126
[4] Sugita Y, Mitsuoka K, Komuro M, Hoshiya H, Kozono Y and Hanazono M 1991 *J. Appl. Phys.* **70** 5977
[5] Sugita Y, Takahashi H, Komuro M, Mitsuoka K and Sakuma A 1994 *J. Appl. Phys.* **76** 6637
[6] Gao C and Doyle W D 1993 *J. Appl. Phys.* **73** 6579
[7] Ortiz C, Dumpich G and Morrish A H 1994 *Appl. Phys. Lett.* **65** 2737
[8] Wallance W E and Huang M Q 1994 *J. Appl. Phys.* **76** 6648
[9] Sun D C, Lin C and Jiang E Y 1995 *J. Phys.: Condens. Matter* **7** 3667
[10] Kim Y K and Narayan P B 1995 *J. Vac. Sci. Technol.* A **13** 1040
[11] Sun D C, Lin C, Jiang E Y and Wu S W 1993 *Thin Solid Films* **260** 1
[12] Ishiwata N, Wakabayashi C and Urai H 1991 *J. Appl. Phys.* **69** 5616
[13] Makino A and Hayakawa Y 1995 *IEEE Trans. Magn.* **31** 3874
[14] Ryu H J, Lee J J, Han S H, Kim H J, Kang I K and Choi J O 1995 *IEEE Trans. Magn.* **31** 3868
[15] Jack K H 1951 *Proc. R. Soc.* A **208** 216
[16] Kopcewicz M, Jagielski J, Gawlik G and Grabias A 1995 *J. Appl. Phys.* **78** 1312